

AZULENE/ALDEHYDE ASSOCIATION: AN ANALOG FOR DAMAGED DNA  
DETECTION

Agne A. Shields

A Senior Honors Project Presented to the

Honors College

East Carolina University

In Partial Fulfillment of the

Requirements for

Graduation with Honors

by

Agne A. Shields

Greenville, NC

December, 2022

Approved by:

Dr. William E. Allen

Chemistry Department

Thomas Harriot College of Arts and Sciences

### **Abstract**

Loss of a nucleic acid base from DNA can leave behind a reactive aldehyde group on ribose. To detect the presence of such “abasic sites,” ethyl-2-aminoazulene-1-carboxylate, a novel azulene-based analog of guanine/adenine, was synthesized. Valeraldehyde was chosen as a simple model for an abasic site.  $^1\text{H}$  NMR kinetics studies with ethyl-2-aminoazulene-1-carboxylate and valeraldehyde show that this is a slow reaction and suggest that it is zero-order with respect to valeraldehyde. This is consistent with a complex mechanism.

## Table of Contents

List of Figures .....	4
List of Tables .....	6
Chapter 1: Introduction .....	7
1.1 DNA Damage: Formation and Significance of Abasic Sites .....	7
1.2 Azulene Based Analog for Purine Bases .....	10
1.3 DNA Open-Form Abasic Site – Aldehyde .....	11
1.4 Kinetics of Association .....	11
Chapter 2: Experimental .....	13
2.1 Synthesis of 2-Tosyloxytropone .....	13
2.2 Synthesis of 2-amino-1,3-diethoxycarbonylazulene .....	13
2.3 Synthesis of 2-amino(ethoxycarbonyl)azulene-1-carboxylic acid ( w/Dioxane and HCl) .....	
2.4 Synthesis of 2-amino(ethoxycarbonyl)azulene-1-carboxylic acid (w/ Acetonitrile) ..	15
2.5 Synthesis of Ethyl-2-aminoazulene-1-carboxylate .....	16
2.6 Kinetics of 1:1 Valeraldehyde and Ethyl-2-aminoazulene-1-carboxylate Association .....	16
Chapter 3: Results .....	18
Chapter 4: Conclusion .....	27

## List of Figures

1.1: Schematic of DNA abasic site formation .....	8
1.2: N-Glycosidic bond is broken in abasic site formation .....	8
1.3: Ethyl-2-aminoazulene-1-carboxylate, a structural analog for adenine and guanine bases .....	10
1.4: The equilibrium between DNA abasic site furanose ring form and open-ring aldehyde form .....	11
1.5: Possible products resulting from the association of ethyl-2-aminoazulene-1-carboxylate and valeraldehyde .....	12
3.1: $^1\text{H}$ NMR peaks of valeraldehyde in a 90:10 DMSO and $\text{D}_2\text{O}$ solution .....	17
3.2: $^1\text{H}$ NMR peaks of ethyl-2-aminoazulene-1-carboxylate and valeraldehyde at 10 minutes .....	18
3.3: $^1\text{H}$ NMR peaks of ethyl-2-aminoazulene-1-carboxylate and valeraldehyde at 17 minutes .....	18
3.4: $^1\text{H}$ NMR peaks of ethyl-2-aminoazulene-1-carboxylate and valeraldehyde at 25 minutes...	19
3.5: $^1\text{H}$ NMR peaks of ethyl-2-aminoazulene-1-carboxylate and valeraldehyde at 33 minutes...	19
3.6: $^1\text{H}$ NMR peaks of ethyl-2-aminoazulene-1-carboxylate and valeraldehyde at 44 minutes...	20
3.7: $^1\text{H}$ NMR peaks of ethyl-2-aminoazulene-1-carboxylate and valeraldehyde at 50 minutes...	20

3.8: $^1\text{H}$ NMR peaks of ethyl-2-aminoazulene-1-carboxylate and valeraldehyde at 58 minutes .....	21
3.9: $^1\text{H}$ NMR peaks of ethyl-2-aminoazulene-1-carboxylate and valeraldehyde at 65 minutes .....	21
3.10: $^1\text{H}$ NMR peaks of ethyl-2-aminoazulene-1-carboxylate and valeraldehyde at 72 minutes .....	22
3.11: Decreasing concentration of ethyl-2-aminoazulene-1-carboxylate over time in a 1:1 (0.0474 mmol: 0.0470 mmol) ethyl 2-aminoazulene-1-carboxylate and valeraldehyde association reaction. ....	23
3.12: Decreasing concentration of ethyl-2-aminoazulene-1-carboxylate over time in a 1:1 (0.04804 mmol: 0.0470 mmol) ethyl 2-aminoazulene-1-carboxylate and valeraldehyde association reaction. ....	23
3.13: Decreasing concentration of ethyl-2-aminoazulene-1-carboxylate over time in a 1:1 (0.04841 mmol: 0.0470 mmol) ethyl 2-aminoazulene-1-carboxylate and valeraldehyde association reaction. ....	24
3.14: Decreasing concentration of ethyl-2-aminoazulene-1-carboxylate over time in a 1:2 ethyl 2-aminoazulene-1-carboxylate and valeraldehyde association reaction. ....	24
3.15: Decreasing concentration of ethyl-2-aminoazulene-1-carboxylate over time in a 1:2.5 ethyl 2-aminoazulene-1-carboxylate and valeraldehyde association reaction. ....	25

3.16: Decreasing concentration of ethyl-2-aminoazulene-1-carboxylate over time in a 1:8 ethyl 2-aminoazulene-1-carboxylate and valeraldehyde association reaction. ....	25
--	----

### **List of Tables:**

3.1: Zero-Order Rate Constants for the Association of Ethyl-2-aminoazulene-1-carboxylate to Valeraldehyde. ....	26
--	----

## Introduction

### 1.1 DNA Damage: Formation and Significance of Abasic Sites

DNA, the carrier of genetic information found within most living organisms, is exposed to numerous forms of damage and gets thousands of lesions daily. An abasic, or apurinic, site is one type of lesion formed by DNA damage. An abasic site is a location on the DNA strand that lacks a pyridine or purine base. Abasic sites may be formed spontaneously through hydrolysis by breaking the deoxyribose and nitrogen base bond. Abasic sites may also be created due to exposure to reactive oxygen species, alkylating agents, and form as intermediates of the base excision repair pathway (1). One of the most common sources of DNA damage is exposure to reactive oxygen species. DNA may be damaged through chemical interaction with these oxygen species, and enzymes repair the resulting damage through the base excision repair pathway from which AP sites may result as intermediates. Below, Figure 1.1 shows a simple schematic of how an abasic site may appear in a DNA sequence. Figure 1.2 displays the change in chemical structure when the n-glycosidic bond is broken, and the purine base is removed.

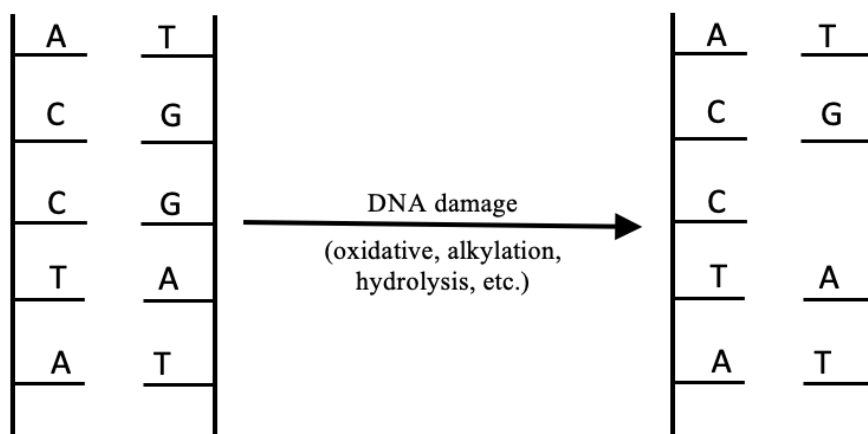


**Figure 1.1: Schematic of DNA abasic site formation.**

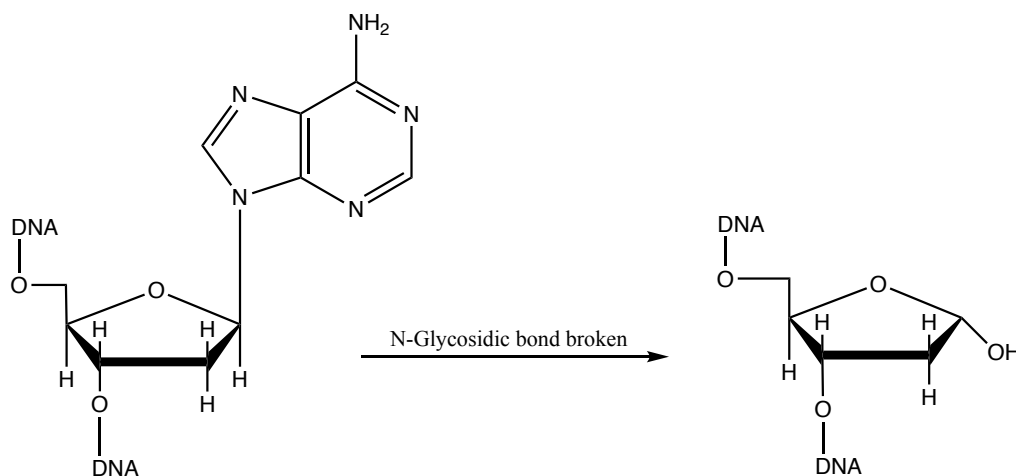


**Figure 1.2: N-Glycosidic bond is broken in abasic site formation.**

Abasic sites may be dangerous lesions as they can lead to numerous problems. If an abasic site is not repaired, it can disrupt DNA replication by blocking function of DNA polymerases, enzymes that drive the replication process (2). The aging process is likely affected by the accumulation of DNA lesions through effects such as further repair inhibition and cell



death. Additionally, mutations can accelerate aging through various genetic diseases such as Hutchinson-Guilford progeria syndrome, Werner syndrome, Fanconi anemia, Alpers-Huttenlocher syndrome, and others (3). Werner syndrome, also known as progeria, usually develops in childhood and its symptoms include alopecia, arthritis, cardiovascular disease, and cataracts.

In addition to disrupting the replication process, abasic sites lead to genetic instability as they are mutagenic and can even lead to cell death. Genetic instability, the higher occurrence of mutations, can be detrimental in some cells as it increases the likelihood of developing driver mutations and promotes cancer growth. Damage of genes coding for tumor suppression proteins responsible for cell cycle arrest or apoptosis, like p53, is particularly insidious (4). The causes of DNA damage and its repair processes are significant points of pharmaceutical interest, as altering them may lead to treatments for the aging process and cancer. Therefore, studying and understanding how, where, and how much damage occurs is essential. Looking at DNA damage can provide insight into how the repair process works and how these processes may be used for further medical uses, such as cancer medications.

There are several methods available to quantify abasic DNA lesions. In one study, liquid chromatography-tandem triple quadrupole mass spectrometry was used in combination with an aldehyde reactive reagent to detect abasic sites (5). However, LC-MS systems are costly and time-intensive to use and maintain. Another commonly used method is the aldehyde reactive probe (ARP) assay which allows the processing of several samples simultaneously. Some drawbacks of ARP assay include the presence of biotin within ARP's chemical structure, which presents difficulties in fluorescent labeling detection methods, and the large size of the ARP

molecule that may hinder its reactivity with abasic sites. The shortcomings of each method and the absence of widely accessible methods in the clinical setting show that more research must be conducted in this field.

## 1.2 Azulene Based Analog for Purine Bases

Azulene is an aromatic isomer of naphthalene consisting of a fused structure of a seven-membered and a five-membered ring – a 10 pi electron system. The ring structure of azulene is similar to the five- and six-membered ring structures of purine bases, making it a potential analog.

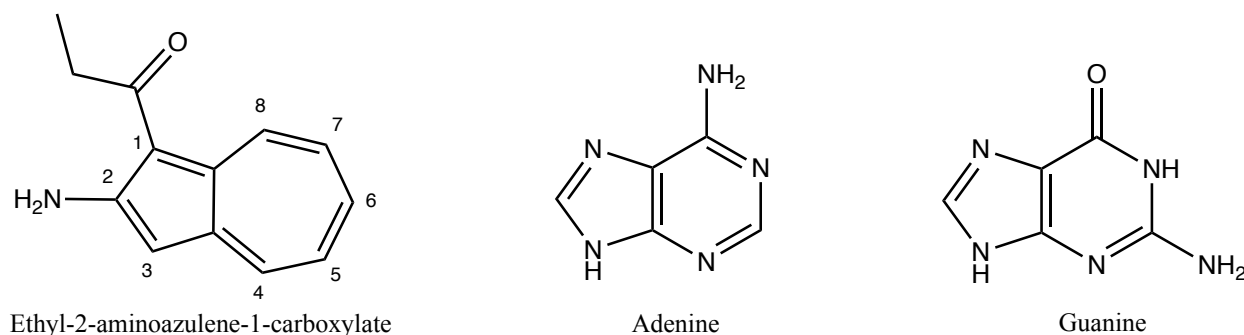


**Figure 1.3: Ethyl-2-aminoazulene-1-carboxylate, a structural analog for adenine and guanine bases**

A 2014 study at Tokyo University discovered that azulene undergoes an electrophilic substitution reaction at the 1- and 3-positions of the molecule due to higher electron density on these carbons. This challenges our previous hypothesis that 2-amino azulene molecules will form a glycosidic bond with deoxyribose through the amine group. Instead, the glycosidic bond may be formed at the 1- and 3- positions of the amino azulene molecule. Additionally, this study

found that the bond formation at the 1- and 3-positions of 2-aminoazulene resulted in a more significant difference in UV-vis spectral absorption bands than when a reaction occurred with the amino group (6).

### 1.3 DNA Open-Form Abasic Site - Aldehyde

DNA lesions are repaired with the base excision repair pathway (BER) – the primary DNA repair pathway. DNA glycosylase recognizes a lesion and breaks the N-glycosidic bond. Breaking of the N-glycosidic bond removes the damaged base, creating an abasic site. In addition to formation due to damage, the base excision repair pathway creates abasic sites as intermediates in the DNA repair process.

The resulting abasic site exists in equilibrium between a furanose ring form and an open-chain aldehyde form. The open chain aldehyde form is highly reactive and thus is susceptible to nucleophilic substitution. Figure 1.4 below shows the equilibrium of the two structural forms of DNA abasic sites.

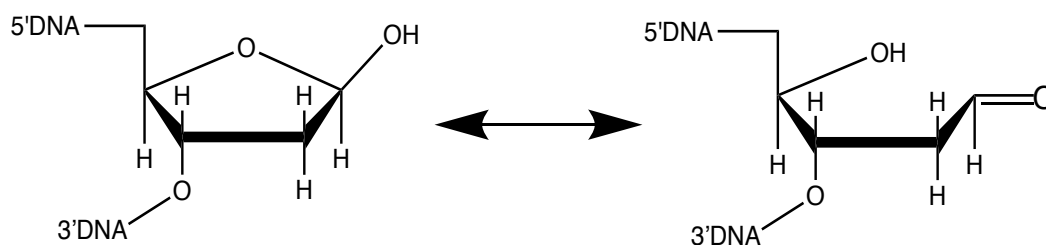


**Figure 1.4: The equilibrium between DNA abasic site furanose ring form and open-ring aldehyde form.**

### 1.4 Kinetics of Association

In this study, the reactive open-ring aldehyde was modeled using a simple, commercially-available aldehyde - valeraldehyde. Ethyl-2-aminoazulene-1-carboxylate was synthesized and used as a purine base analog. Figure 1.5 below displays potential products resulting from the association of ethyl-2-aminoazulene-1-carboxylate and valeraldehyde.

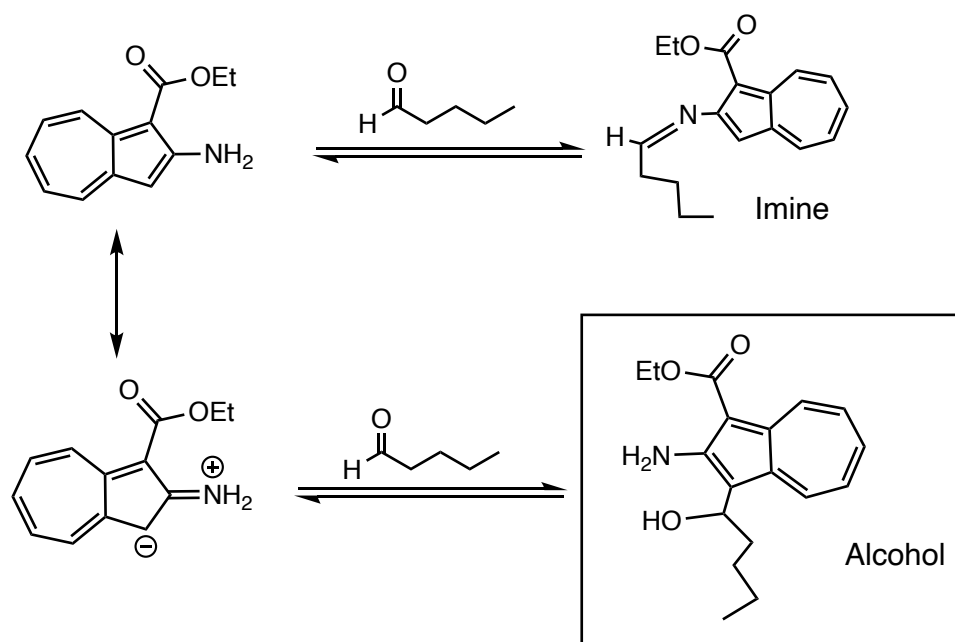


**Figure 1.5: Possible products resulting from the association of ethyl-2-aminoazulene-1-carboxylate and valeraldehyde.**

To begin developing an abasic site detection model we chose to study the kinetics of the association reaction under favorable (i.e., relatively highly-concentrated) conditions. The study of reaction rates will provide insights in future studies on how to optimize the rate of the reaction, and reduce the production of byproducts.

To study the reaction kinetics for the association of valeraldehyde and ethyl-2-aminoazulene, proton nuclear magnetic resonance (NMR) was employed. NMR has the ability to

detect signals of individual atoms as well as monitor the change in these signals, making it a useful tool for analyzing reaction kinetics. Some limitations of NMR include greater time requirements for data collection, and relatively low sensitivity. These limitations would be problematic for rapid reactions. However, the slow reaction time for the aldehyde association reaction makes NMR a suitable choice.

## **Experimental:**

### **2.1 Synthesis of 2-tosyloxypone**

Tropolone (32.93 mmol) was combined with pyridine (11.0 mL, 136.0 mmol) in the reaction flask forming a clear yellow-tinted solution. The solution was capped and placed to stir in an ice bath. After approximately ten minutes, TsCl (32.28 mmol) added slowly to the solution. The solution became light-cream colored and two layers formed. After approximately twenty minutes of stirring in the ice bath, the reaction flask was removed and left capped to stir overnight. After ~25 hours of stirring, the reaction was stopped. The reaction mixture was tan-brown, clay-like mixture. The mixture was diluted with ice-cold ddH<sub>2</sub>O (~30 mL) and swirled. The precipitate was collected using suction filtration (20  $\mu$  fine frit), washed ice-cold ddH<sub>2</sub>O (4 x ~10 mL), and left over suction for about thirty minutes. The product was placed under vacuum to dry overnight. Mass and percent yield measurements were obtained for the solid. The mass of the isolated product was found to be 8.92 g resulting in a 98.0% yield.

### **2.2 Synthesis of 2-amino-1,3-diethoxycarbonylazulene**

2-Tosyloxypone (16.4 mmol) was added to ethanol (200 proof, ~80.5 mL) to form a light tan suspension. A stir bar was added to the suspension, and the reaction flask was set to stir

in an ice bath. Ethyl cyanoacetate (1.061 mmol) and t-butylamine (0.6969 mmol) were added to the suspension. After the addition of t-butylamine, the reaction mixture became bright orange. The reaction mixture was left to stir in the ice bath and slowly reach room temperature. After about 20 hours of stirring, the solution was dark red and a grainy, orange precipitate was visible. The reaction mixture was diluted with ddH<sub>2</sub>O (~30 mL) was then filtered using suction filtration (10-15  $\mu$  frit). The solid was washed with ddH<sub>2</sub>O. After washing with ddH<sub>2</sub>O, an orange precipitate formed in the filtrate. The filtrate was reduced to about half of its original volume and diluted with ddH<sub>2</sub>O (~55 mL). The filtrate was then placed in a refrigerator to cool. After about 40 minutes of cooling, the filtrate containing precipitate was filtered using suction filtration (30  $\mu$  frit) and washed with ddH<sub>2</sub>O. The isolated precipitate was a thick, clay-like solid. Both crops were placed under vacuum to dry. Mass and percent yield measurements were obtained for each crop. The mass of the first crop was found to be 1.31 g and the mass of the second crop was found to be 2.73 g, resulting in an 85.8% yield.

### **2.3 Synthesis of 2-amino(ethoxycarbonyl)azulene-1-carboxylic acid (w/dioxane and HCl)**

2-Amino-1,3-diethoxycarbonylazulene (2.510 mmol) was dissolved in dioxane (19 mL) along with ddH<sub>2</sub>O (10.0 mL) and NaOH (5.295 mmol), forming a clear bright orange solution. A stir bar was added and the reaction flask was attached to a water-cooled condenser and placed on a heating mantle (set to 59). The solution was left to stir at reflux overnight. After about 21.5 hours of stirring at reflux, the solution was removed from heat and allowed to cool. The solution was a dark reddish-brown. The reaction solution was poured over a mixture of 5% HCl and crushed ice (~100 mL) and a bright yellow precipitate formed immediately. The mixture was left to sit at room temperature until all ice was melted. Once ice was melted, the precipitate was

isolated using suction filtration and was washed with ddH<sub>2</sub>O. The isolated solid was allowed to dry over suction for about 30 minutes. The product was then placed under vacuum to dry. Once dry, mass and percent yield measurements were obtained. The mass of the isolated solid was found to be 465.7 mg, resulting in a 71.6% yield.

#### **2.4 Synthesis of 2-amino(ethoxycarbonyl)azulene-1-carboxylic acid (w/acetonitrile)**

2-Amino-1,3-diethoxycarbonylazulene (2.1332 mmol), acetonitrile (15.0 mL), and ddH<sub>2</sub>O (10.00 mL) were combined in a reaction flask, forming an orange/brown suspension. NaOH (7.126 mmol) and a stir bar were added to the suspension. The reaction flask was then placed to stir over heat. After about three minutes of stirring over heat, the reagents dissolved and formed a red-orange solution. An air-cooled condenser was attached to the reaction flask and the solution was allowed to reach reflux. After about 18 hours of stirring at reflux, the reaction flask was removed from heat and allowed to cool to room temperature. The solution had become red-brown and was then treated with glacial acetic acid (0.5 mL) and gently swirled. After the addition of acid, yellow precipitate began to form. The reaction flask was then capped and left to sit overnight. The next day, suction filtration was performed to isolate the precipitate. The isolated solid was washed with ddH<sub>2</sub>O and an orange precipitate formed in the filtrate. The first crop of isolated solid was placed under vacuum to dry. Suction filtration was performed on the filtrate and the isolated orange-brown solid was washed with ddH<sub>2</sub>O. The second crop was placed under vacuum to dry. <sup>1</sup>H NMR analysis showed that the second crop was too impure containing some unreacted starting material and waste products, therefore the second crop was discarded. The mass of the first crop was 296.5 mg, resulting in a 53.6% yield.

## 2.5 Synthesis of ethyl-2-aminoazulene-1-carboxylate

2-Amino(ethoxycarbonyl)azulene-1-carboxylic acid (0.7811 mmol) was combined with  $\text{H}_3\text{PO}_4$  in a pressure tube forming a dark yellow suspension. Once a stir bar was added and the pressure tube was capped, it was placed in a hot oil bath set to 93 °C and stirred. Gas bubbles began forming after about a minute of heating; after about three minutes of heating the solution was black-brown. The pressure tube was removed from heat after one hour and was allowed to cool. The reaction mixture was then poured into ice water immediately producing an orange-brown precipitate. A black oil-like substance was present at the bottom of the solution, but went back into solution with some stirring. The ice mixture was left in the refrigerator overnight to allow the ice to melt slowly. After about 20 hours in the refrigerator, the precipitate had settled to the bottom of the beaker. The mixture was centrifuged and the top layer was decanted. The remaining solid pellets were left to dry. Mass and percent yield measurements were obtained. The mass was found to be 86.7 mg, resulting in a 51.6% yield.

## 2.6 Kinetics of 1:1 valeraldehyde and ethyl-2-aminoazulene-1-carboxylate association

Valeraldehyde (0.0470 mmol),  $\text{D}_2\text{O}$  (0.083 mL), DMSO (0.75 mL), and glacial acetic acid (0.00939 mmol) were combined in an NMR tube. A  $^1\text{H}$ NMR spectrum was acquired. Then ethyl-2-aminoazulene-1-carboxylate (0.0474 mmol) was added forming a dark brown solution. NMR analysis was performed with repeating scans every 5-10 minutes. Association of valeraldehyde and ethyl-2-aminoazulene-1-carboxylate was followed by observing the decrease in intensity (integral) of the singlet representing the hydrogen on the azulene 3-carbon.



## Results

In this study, the kinetics of association between ethyl-2-aminoazulene-1-carboxylate and valeraldehyde were studied using  $^1\text{H}$  NMR. Two sets of conditions were analyzed in triplicate. The first study was with a 1:1 ratio of ethyl-2-aminoazulene-1-carboxylate and valeraldehyde and the second was of a 1:2 ratio of ethyl-2-aminoazulene-1-carboxylate and valeraldehyde. For each study, after all reagents except ethyl-2-aminoazulene-1-carboxylate were added, a  $^1\text{H}$  NMR scan of the solution was obtained – an example of which can be seen Figure 3.1 below. Once the initial  $^1\text{H}$  NMR scan was obtained, ethyl-2-aminoazulene-1-carboxylate was added to the NMR solution and  $^1\text{H}$  NMR analysis was resumed with repeating scans every 5-10 minutes. An example data set from a 1:1 ethyl-2-aminoazulene-1-carboxylate and valeraldehyde kinetics study is shown in Figures 3.2 to 3.10 below.

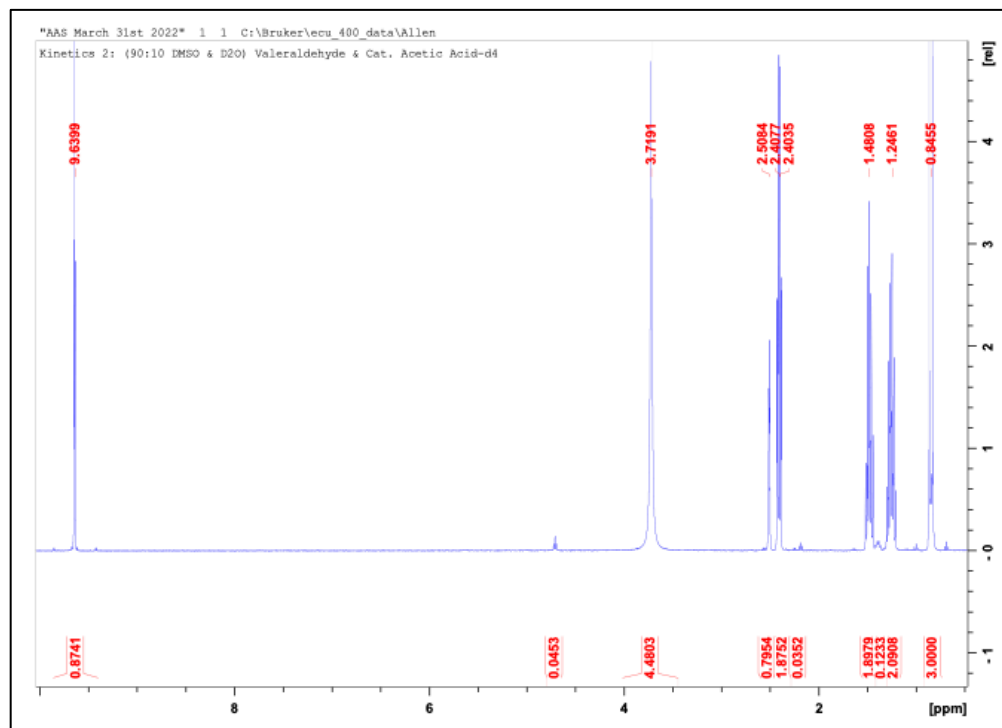


**Figure 3.1:**  $^1\text{H}$  NMR peaks of valeraldehyde in a 90:10 DMSO and  $\text{D}_2\text{O}$  solution.

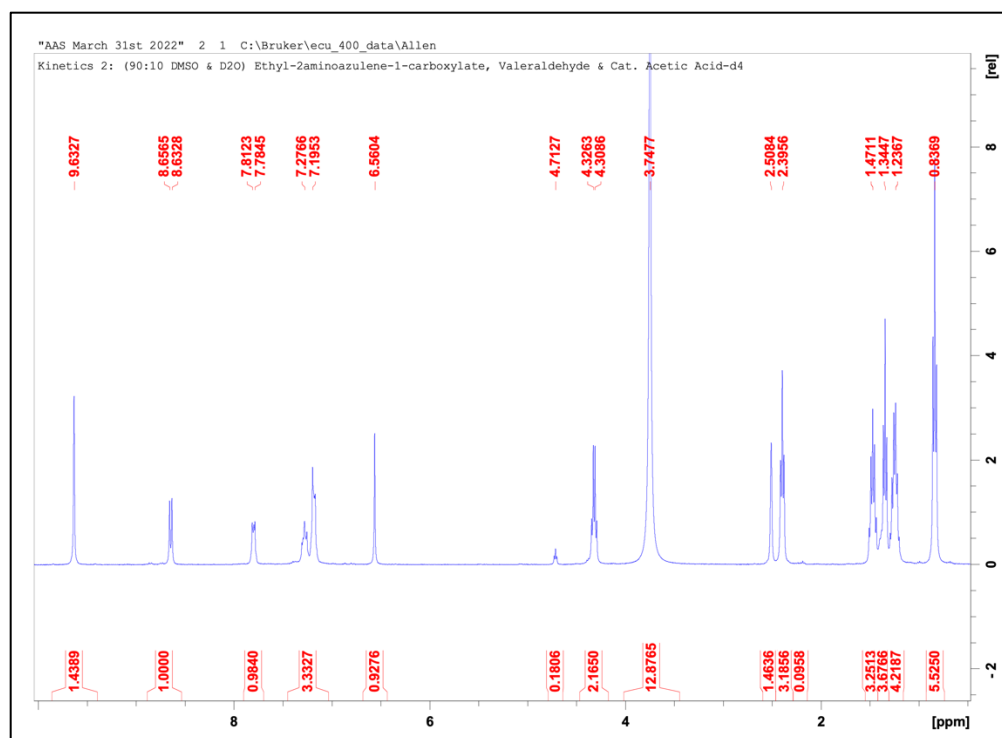


Figure 3.2:  $^1\text{H}$  NMR peaks of ethyl-2-aminoazulene-1-carboxylate and valeraldehyde at 10 minutes.

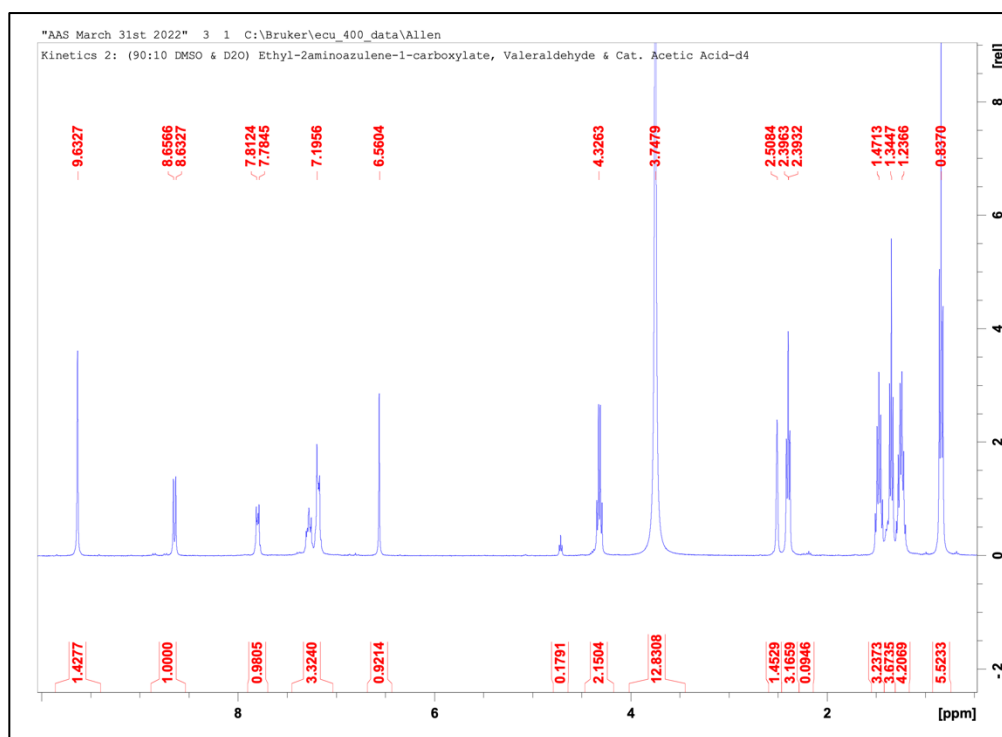


Figure 3.3:  $^1\text{H}$  NMR peaks of ethyl-2-aminoazulene-1-carboxylate and valeraldehyde at 17 minutes.

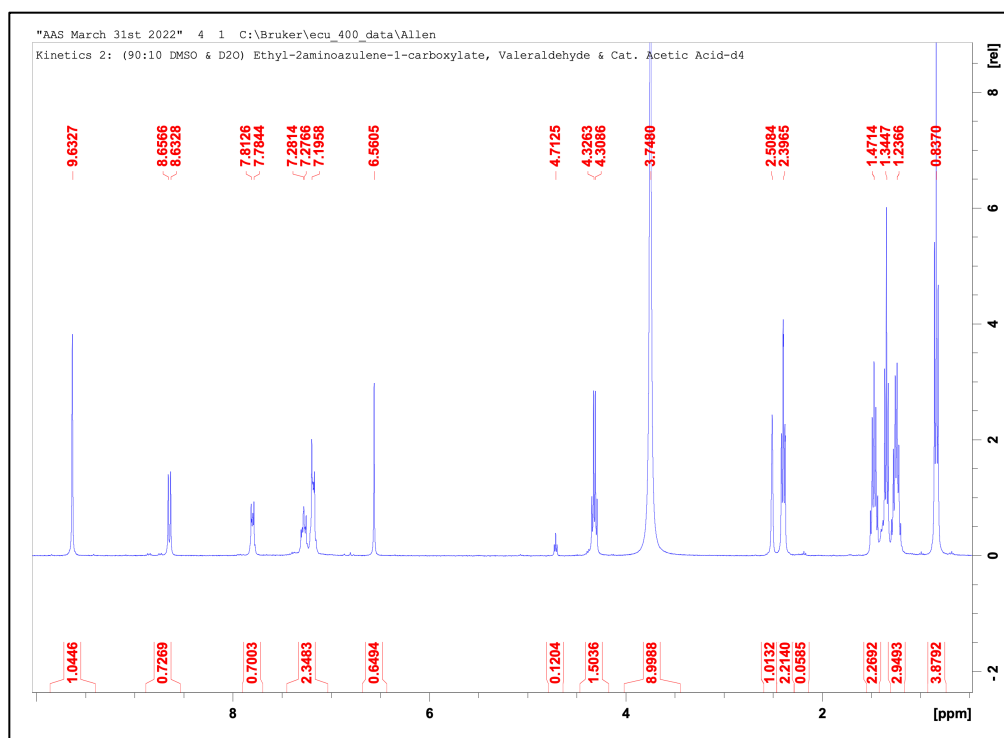


Figure 3.4:  $^1\text{H}$  NMR peaks of ethyl-2-aminoazulene-1-carboxylate and valeraldehyde at 25 minutes.

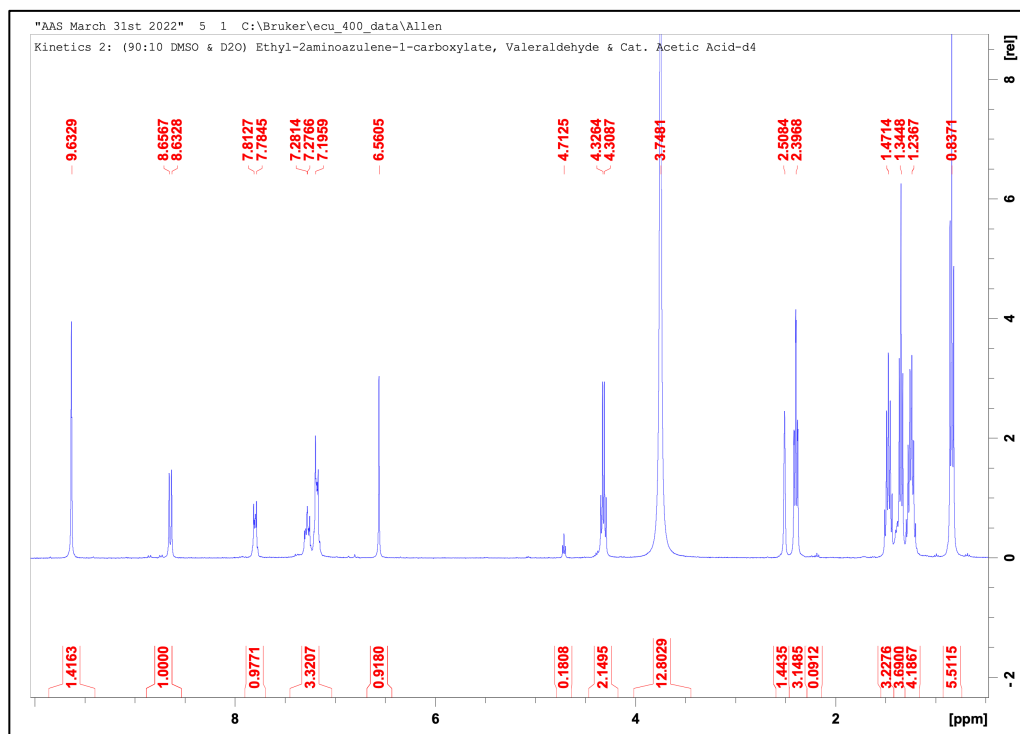


Figure 3.5:  $^1\text{H}$  NMR peaks of ethyl-2-aminoazulene-1-carboxylate and valeraldehyde at 33 minutes.

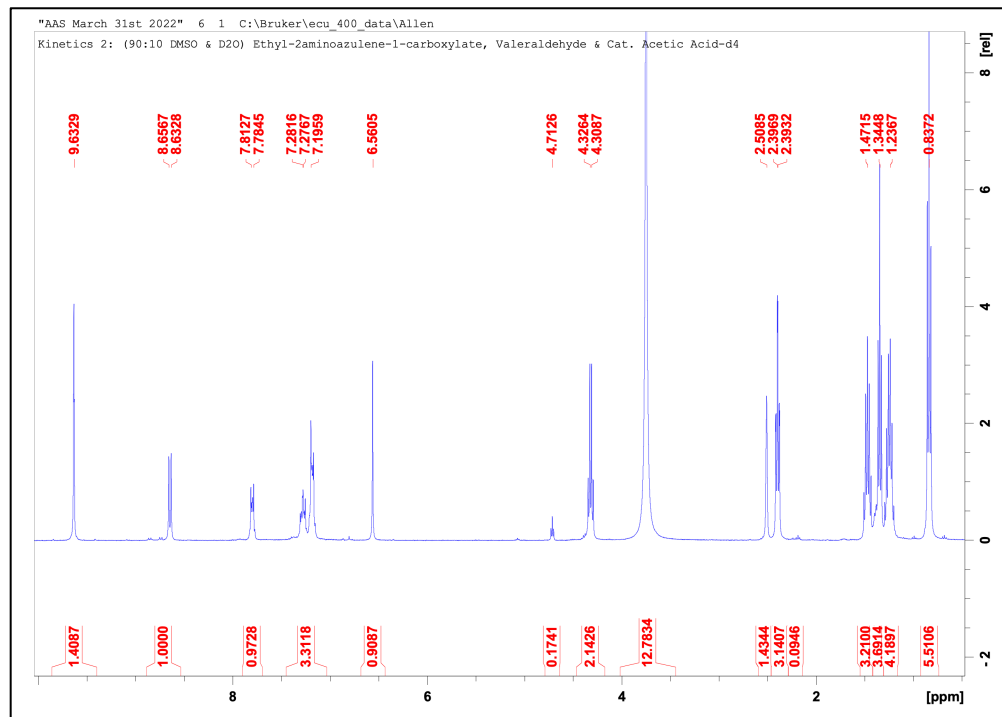


Figure 3.6:  $^1\text{H}$  NMR peaks of ethyl-2-aminoazulene-1-carboxylate and valeraldehyde at 44 minutes.

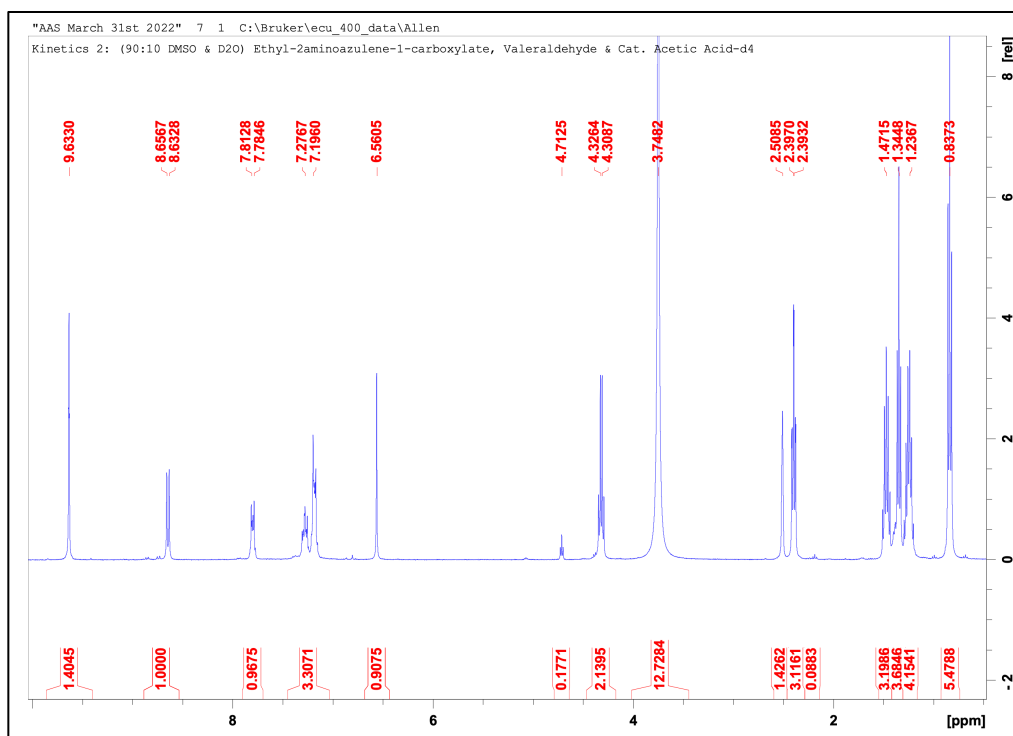


Figure 3.7:  $^1\text{H}$  NMR peaks of ethyl-2-aminoazulene-1-carboxylate and valeraldehyde at 50 minutes.

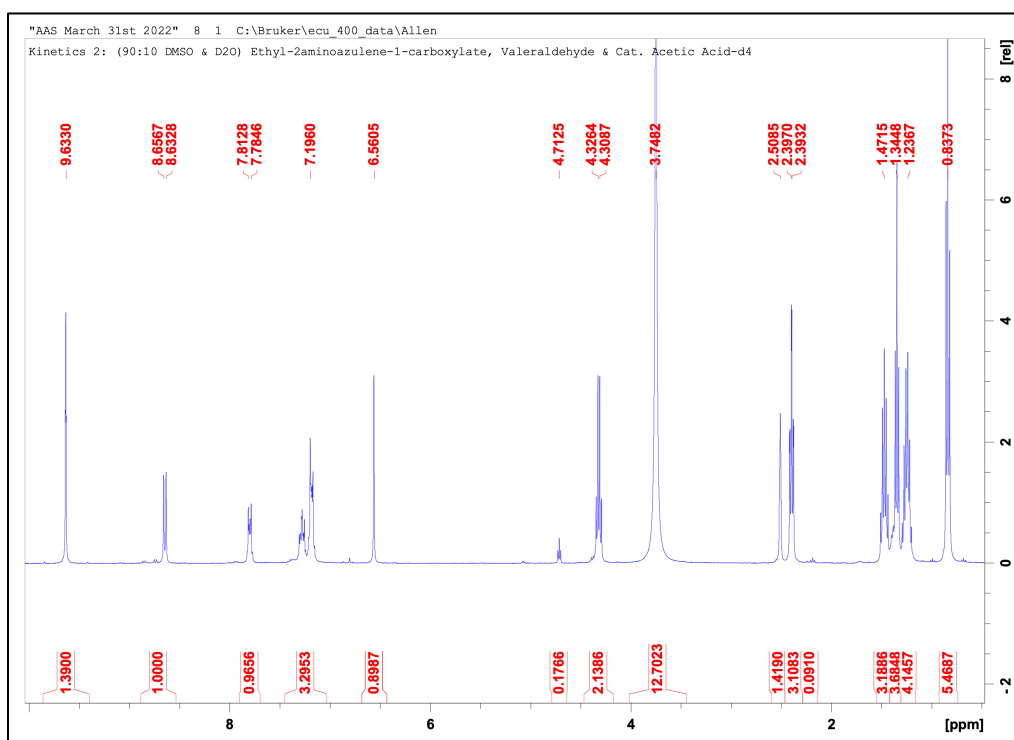


Figure 3.8:  $^1\text{H}$  NMR peaks of ethyl-2-aminoazulene-1-carboxylate and valeraldehyde at 58 minutes.

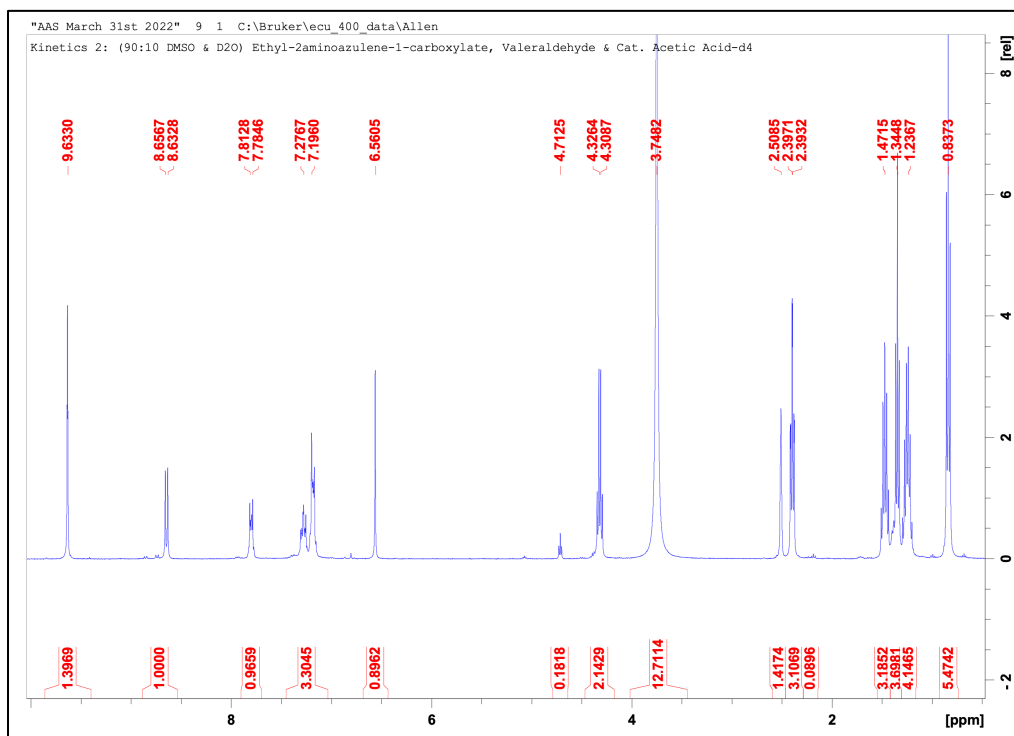


Figure 3.9:  $^1\text{H}$  NMR peaks of ethyl-2-aminoazulene-1-carboxylate and valeraldehyde at 65 minutes.

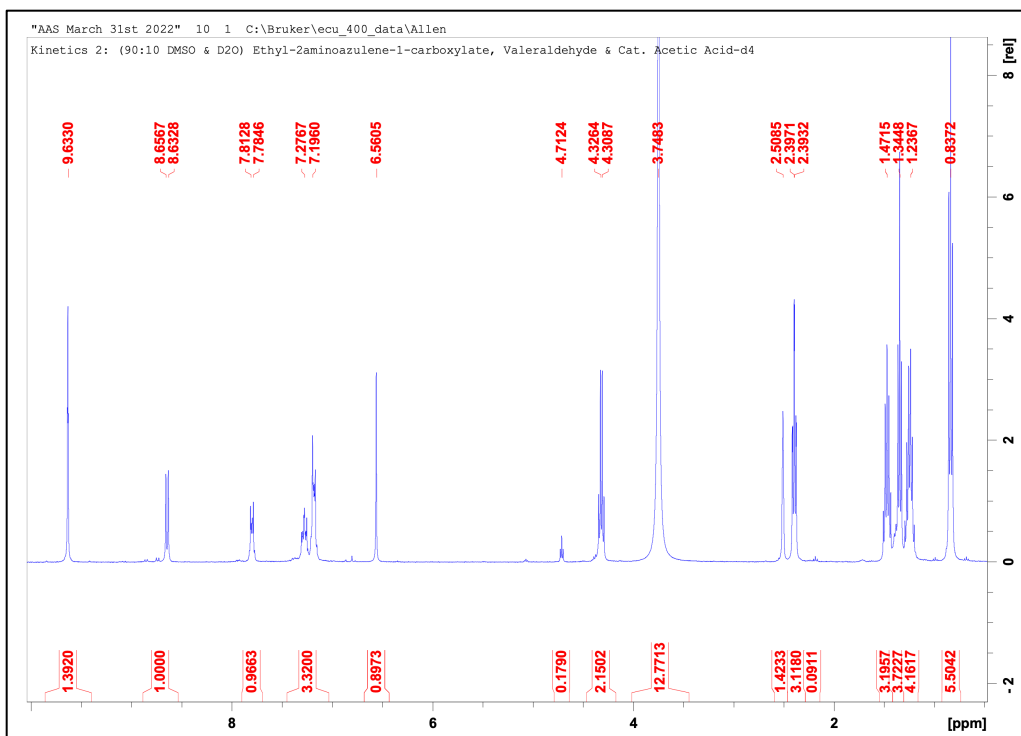
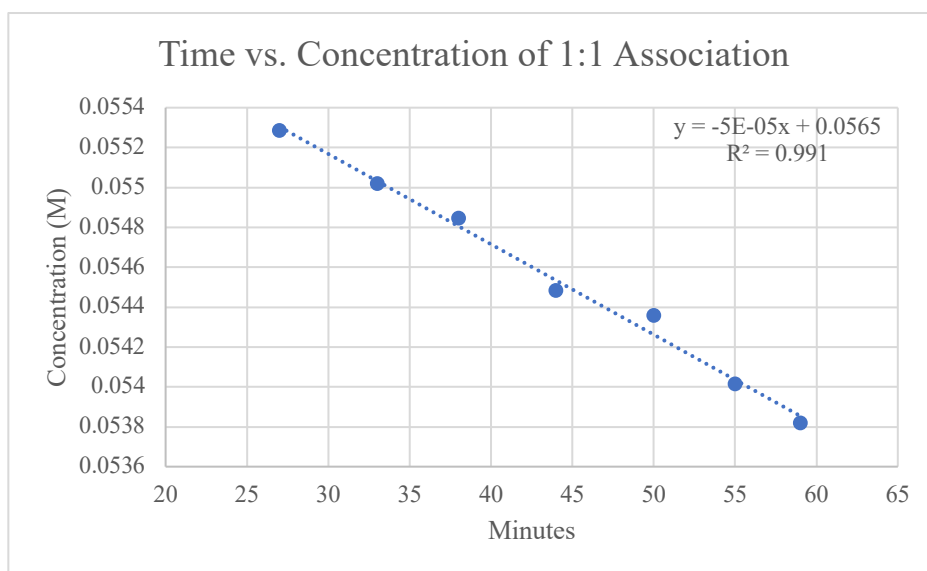


Figure 3.10:  $^1\text{H}$  NMR peaks of ethyl-2-aminoazulene-1-carboxylate and valeraldehyde at 72 minutes.

### Rate Constant Determination

The peak integral representing the hydrogen on carbon three (as shown in Figure 1.2) of ethyl-2-aminoazulene-1-carboxylate is proportional to the molar concentration of unreacted ethyl-2-aminoazulene-1-carboxylate. Therefore, recording the change in concentration of unreacted ethyl-2-aminoazulene-1-carboxylate over time would allow the rate constant of the association reaction to be determined.



**Figure 3.11: Decreasing concentration of ethyl-2-aminoazulene-1-carboxylate over time in a 1:1 (0.0474 mmol: 0.0470 mmol) ethyl 2-aminoazulene-1-carboxylate and valeraldehyde association reaction.**

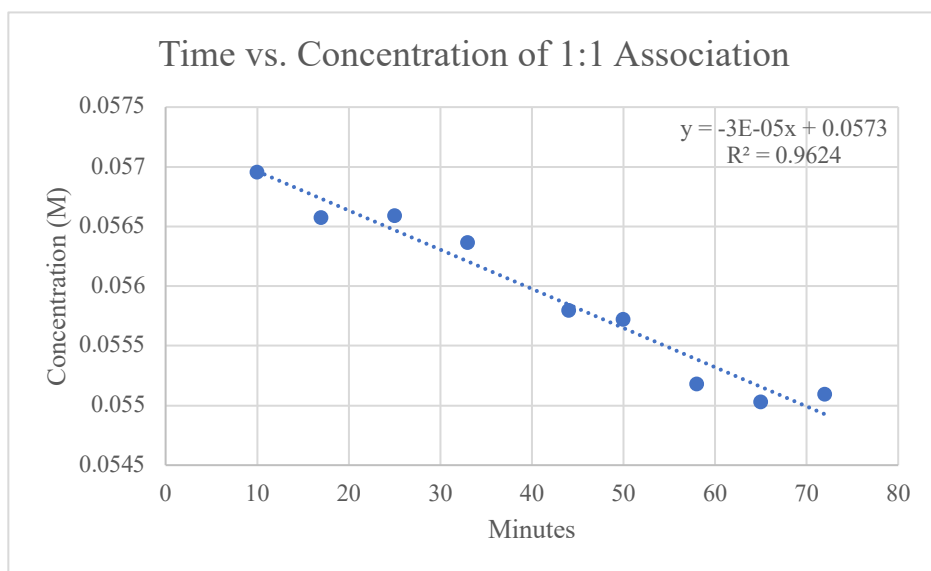


**Figure 3.12: Decreasing concentration of ethyl-2-aminoazulene-1-carboxylate over time in a 1:1 (0.04804 mmol: 0.0470 mmol) ethyl 2-aminoazulene-1-carboxylate and valeraldehyde association reaction.**

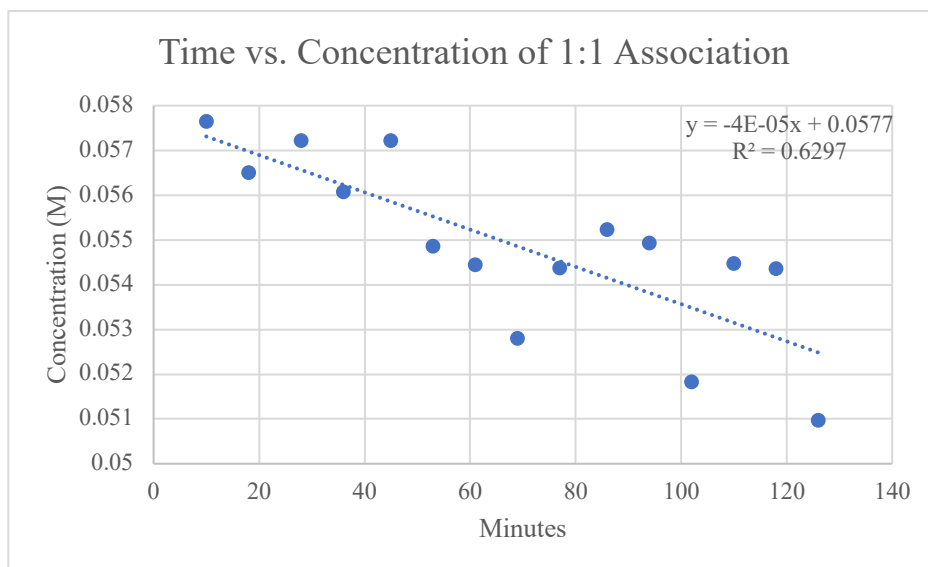


**Figure 3.13: Decreasing concentration of ethyl-2-aminoazulene-1-carboxylate over time in a 1:1 (0.04841 mmol: 0.0470 mmol) ethyl 2-aminoazulene-1-carboxylate and valeraldehyde association reaction.**

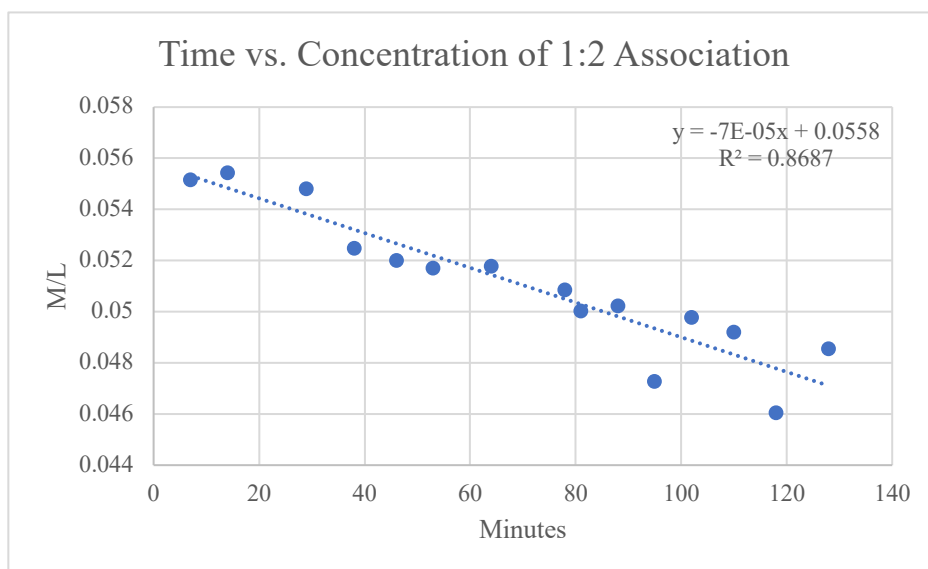


**Figure 3.14: Decreasing concentration of ethyl-2-aminoazulene-1-carboxylate over time in a 1:2 ethyl 2-aminoazulene-1-carboxylate and valeraldehyde association reaction.**



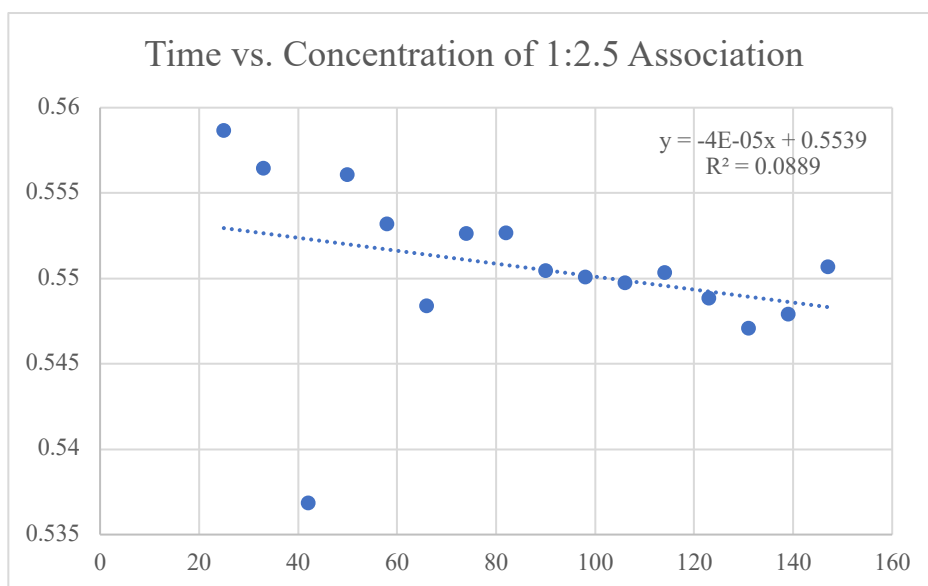


**Figure 3.15: Decreasing concentration of ethyl-2-aminoazulene-1-carboxylate over time in a 1:2.5 ethyl 2-aminoazulene-1-carboxylate and valeraldehyde association reaction.**

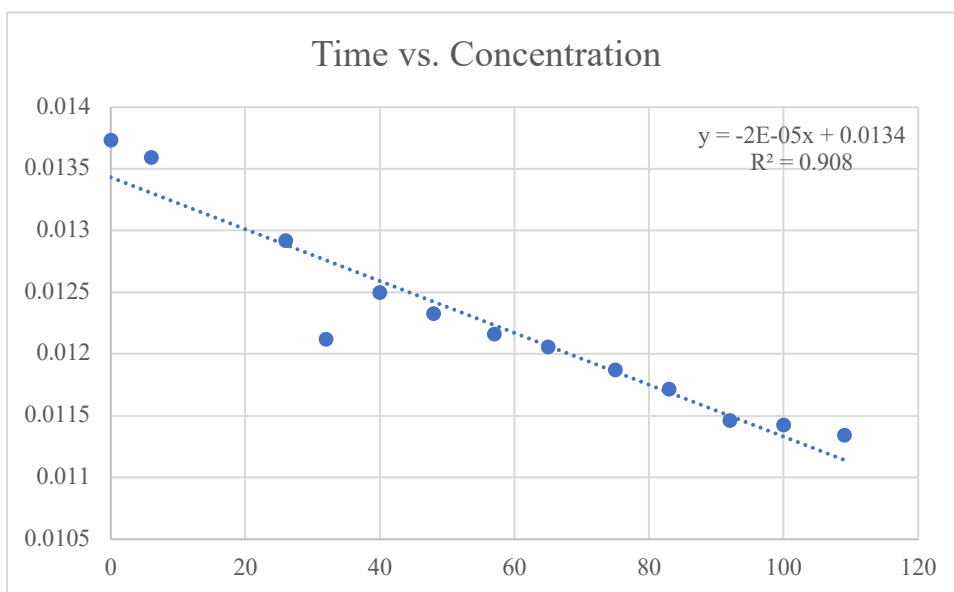


**Figure 3.16: Decreasing concentration of ethyl-2-aminoazulene-1-carboxylate over time in a 1:8 ethyl 2-aminoazulene-1-carboxylate and valeraldehyde association reaction.**

A 1:1 kinetics study was repeated in triplicate and the graphical results of ethyl-2-aminoazulene-1-carboxylate suggest that the association reaction between ethyl-2-aminoazulene-1-carboxylate and valeraldehyde is zero-order – *i.e.*, independent of concentration of the aldehyde. Subsequent kinetics studies were performed at stoichiometric ratios of 1:2, 1:2.5, and 1:8.

**Table 3.1: Zero-Order Rate Constants for the Association of Ethyl-2-aminoazulene-1-carboxylate to Valeraldehyde.**

Ratio of Azulene to Valeraldehyde	Rate of Association (k)
1:1 (average)	3.99E-05
1 to 2	6.79E-05
1 to 2.5	3.79E-05
1 to 8	2.10E-05

The 1:1 kinetics study of ethyl-2-aminoazulene-1-carboxylate association with valeraldehyde suggested that the reaction between the two reagents was zero-order – the rate did not change with varying concentrations of reactants. To confirm that the rate was zero-order with respect to valeraldehyde, subsequent 1:2, 1:2.5, and 1:8 kinetics studies were performed. Each study yielded a similar  $10^{-5}$  rate constant.

## Conclusions

$^1\text{H}$  NMR experiments in DMSO-water show the reaction to be zero-order with respect to the concentration of valeraldehyde. However, the small absolute rate constant ( $k = 4 \times 10^{-5} \text{ min}^{-1}$ ) will likely render this approach impractical for clinical deployment. Unfortunately, due to the

small rate constant and long reaction time,  $^1\text{H}$  NMR studies did not prove to be sensitive enough to accurately detect changes in reactant concentration over time. Future studies could involve continuing kinetics studies of azulene and aldehyde association while varying azulene concentrations to confirm the overall association reaction order.

## References

- (1) Katerji, Meghri, and Penelope J Duerksen-Hughes. "DNA Damage in Cancer Development: Special Implications in Viral Oncogenesis." *American Journal of Cancer Research*, vol. 11, no. 8, 15 Aug. 2021.
- (2) Thompson, Petria S., and David Cortez. "New Insights into Abasic Site Repair and Tolerance." *DNA Repair*, vol. 90, 30 Apr. 2020, p. 102866.,  
<https://doi.org/10.1016/j.dnarep.2020.102866>.
- (3) Yousefzadeh, Matt, et al. "DNA Damage—How and Why We Age?" *ELife*, vol. 10, 29 Jan. 2021, <https://doi.org/10.7554/elife.62852>.
- (4) Ozaki, Toshinori, and Akira Nakagawara. "Role of p53 in Cell Death and Human Cancers." *Cancers* vol. 3,1 994-1013. 3 Mar. 2011, doi:10.3390/cancers3010994
- (5) Rahimoff, René, et al. "5-Formyl- and 5-Carboxydeoxycytidines Do Not Cause Accumulation of Harmful Repair Intermediates in Stem Cells." *Journal of the American Chemical Society*, vol. 139, no. 30, 17 July 2017, pp. 10359–10364.,  
<https://doi.org/10.1021/jacs.7b04131>.
- (6) Nakagawa, Hajime, et al. "Unexpected Formation of 2-Amino-(1-(2-Nitrophenylsulfinyl)Azulene by the Reaction of 2-Aminoazulene with 2-Nitrobenzenesulfonyl Chloride." *Heteroatom Chemistry*, vol. 25, no. 5, 29 Oct. 2014, pp. 389–395., <https://doi.org/10.1002/hc.21173>.